Bakker A., Marshall E.M. (1992) Laminar Mixing with Kenics In-Line Mixers. Proceedings of the Fluent Inc.'s Users Group Meeting, October 13-15, 1992, Burlington, Vermont, page 126-146.

LAMINAR MIXING WITH KENICS IN-LINE MIXERS

André Bakker

Chemineer, Inc.
5870 Poe Avenue
Dayton, OH 45401

&

Elizabeth M. Marshall

Fluent, Inc.
Centerra Resource Park
10 Cavendish Court
Lebanon, NH 03766

Presented at the:

Fluent Inc.'s 1992 Users' Group Meeting
October 13-15, 1992
Burlington, Vermont

ABSTRACT

The flow pattern, pressure drop and the mixing characteristics of Kenics static mixers are investigated by means of computer simulations with Fluent V4.10.

The simulations gave new insights in the flow pattern in the helical mixing elements. The pressure drop predictions compare favorably with literature data. Mixing in the elements occurs through a combination of flow splitting and shearing at the junctions of successive elements and a stretching and folding mechanism within the elements. This makes the Kenics element an excellent radial mixing device.

I. INTRODUCTION

Mixing is an operation commonly encountered in the chemical process industries. Often used mixing devices are dynamic mixers for agitated tanks and static mixers for pipe line mixing, such as manufactured by Chemineer Inc. The Kenics helical mixing element is mainly used for in-line blending of liquids under laminar flow conditions. Other types of static mixers are available for turbulent operating conditions and gas-gas mixing.

The Kenics in-line mixer (Figure 1) consists of a number of elements of alternating right and left hand 180° helices. The elements are positioned such that the leading edge of an element is perpendicular to the trailing edge of the next element. The length of the elements is one and a half tube diameters.

Kenics in-line mixers have been used in the chemical process industries for about 25 years. Most of the experimental work concentrated on establishing design guidelines and pressure drop correlations ([1]-[5]). The number of investigations to the flow and the mixing mechanisms is limited, probably due to experimental difficulties. The recent advancements in Computational Fluid Dynamics (CFD) have raised the question to which extent computer simulations can be used as a tool in the design and analysis of static mixers.

This work has two objectives. The first objective is to explore the possibilities Computational Fluid Dynamics offers in the analysis of mixing induced by helical elements. The second objective is to gain insight in the mixing mechanism in Kenics static mixers. To meet these objectives the flow pattern, pressure drop and mixing characteristics of Kenics in-line mixers are analyzed by means of computer simulations with Fluent V4.10.

The paper describes the numerical model, the calculated flow pattern and the mixing of two chemical species.

II. NUMERICAL MODEL

II.A. Geometry

The model consisted of a body fitted grid of 20x20x242 = 96,800 grid nodes. The grid was generated with Fluent PreBFC V4.01 and exported to Fluent V4.10 for performing the flow and mixing computations. The helical elements were modelled by blocking the flow with "wall cells". Each element had a thickness of two wall cells.

Fluid entered the tube through "inlet cells" at the inlet. A uniform velocity profile

with velocities of 0.01 m/s was prescribed. The outlet of the tube was modelled by means of zero gradient boundary conditions for all flow variables.

In the computations the tube had a diameter of 0.02 m and a length of 0.24 m. The tube was equipped with six 180° elements with a length of 0.03 m each. There was an empty piece of tube at the beginning and at the end with a length of one element. The thickness of the elements was 0.04 times the tube diameter. The density of the liquid was 1000 kg/m^3. The liquid viscosity was 0.02 Pa.s. The Reynolds number was Re = 10.

To evaluate the mixing in the tube the transport of two chemical species, named white and black, was calculated. The binary diffusion coefficient of the two species was D = 1.5E-9 m^2/s. This is the diffusion coefficient of saline solution in water. The center of the inlet was 100% white; the outside of the inlet was 100% black.

II.B. Solution Method

The model turned out to be difficult to converge. A lot of runs were made with different settings of the solution parameters and with small variations in the model set-up to find out which settings gave the most stable solution process.

Starting the computation with a relatively accurate initial guess for the flow field had a positive effect on the stability of the solution. An initial guess was made by patching all the tangential velocities (here tangential means parallel to the grid lines in the direction of the tube) with the same velocity as prescribed in the inlet of the tube.

The flow rates on both sides of the elements should be equal due to the symmetry of the design. Fluent will only predict a symmetrical flow pattern when the static mixing elements have a thickness of at least two cells. When the element is only one cell thick, the flow impinging on the element edge has to split between the two sides of the element in this one cell, and the split may not be even. For the correct modelling of the flow division, at least two cells are necessary.

The flow field was calculated using the power-law numerical interpolation scheme. This flow field was then used as a basis for calculating the transport of the two chemical species in the tube. To minimize the effect of false, numerical diffusion on the predicted mixing rate the QUICK numerical interpolation scheme was used in these calculations. Numerical diffusion is the smearing out of gradients due to interpolation errors or due to a too coarse grid. Numerical diffusion is less with the Quick scheme than with the Power Law interpolation scheme [6]. A disadvantage of using Quick is that the computation time is much longer.

The computations were performed on a SUN-SPARC II workstation, equipped with 32 Megabytes of RAM, 128 Megabytes swap space and a total hard-disk capacity of 1.7 Gigabytes. Reaching a converged solution for both the flow field and the concentration field took about 1000 iterations which, with this grid size, accounts for about a week of computation time.

III. RESULTS

III.A. Flow Pattern

Figure 2 shows a raster plot of the velocity magnitude at various intersections in a tube equipped with six 180° elements. White denotes high velocities and black denotes low velocities.

At the inlet a flat velocity profile is prescribed. This profile rapidly develops into a parabolic velocity profile with higher velocities in the center then at the wall. High speed cores are formed. The high speed cores are split up at the flow divisions, resulting in four cores, arranged in a flower like pattern. Within every element those four cores merge and form two high speed cores again, one on each side of the element. Note that near the end of the elements the high speed cores are located in the corners and not in the center. The highest velocities are found more near the corners, just before the junctions. The swirl of the fluid forces more fluid to enter the next element on the downstream side than on the upstream side of the flow division.

Figures 3a,b show the projections of the velocity vectors at various intersections within the tubes. Figure 3b shows the velocities near a flow division.

Wilkinson and Cliff [1] state that there is a significant amount of fluid circulation within the elements (Fig. 4). The flow simulations show that this is not the case. All the liquid velocities are directed along the helical blade, except near the junctions, where some circulation occurs. Fluid moving within an element does not circulate. However, there is a relative motion between the helical blade and the fluid due to the fact that, depending on the position, the blade will twist away or towards the fluid when the fluid is moving axially through the tube. To get an impression of this relative motion a coordinate transformation to the helical reference frame has been performed, making use of the Fluent User Subroutines option. The velocities in the helical reference frame are given by:

$$u_{hr} = u - \frac{T}{l}\langle w\rangle\sqrt{x^2+y^2}\cos\left[atan\left(\frac{y}{x}\right)\right]$$

$$v_{hr} = v + \frac{T}{l}\langle w\rangle\sqrt{x^2+y^2}\sin\left[atan\left(\frac{y}{x}\right)\right] \qquad (1)$$

Here u and v are the velocities in the x and y directions respectively, relative to a cartesian frame of reference; u_{hr} and v_{hr} are the corresponding velocities in the helical reference frame; $\langle w\rangle$ is the average velocity in the z direction (cartesian reference frame, parallel with the tube); T is the twist of the element in radians and l is the length of the element.

Figure 5 shows both the absolute velocities (left, cartesian frame of reference) and the relative velocities (right, helical reference frame). The blade is twisted in the clockwise direction. This figure illustrates that, although there is no real circulation, the position of fluid clumps will shift relative to the blade while the fluid moves through the mixer.

III.B. Pressure Drop

Figure 6 shows the pressure drop as a function of the position in the tube, z/D. Here z is the axial coordinate (0 at the inlet) and D is the tube diameter.

The pressure drop across the elements was calculated with the correlation proposed in the KTEK-series [7] for laminar flow, which forms the basis for the Kenics design procedures:

$$\Delta p = (K'_{OL}A + K_{OL})\frac{64}{Re}\frac{L}{D}\frac{1}{2}\rho\langle w\rangle^2 \qquad (2)$$

The various parameters used in Equation (2) are listed in table 1. For reasons of comparison the pressure drop was also calculated with various literature correlations. The predicted pressure drops are listed in table 2.

The pressure drop predicted by the Kenics design procedure and predicted by Fluent are within 10%, thus giving confidence in the results. There is a large variation in the pressure drop calculated by the literature correlations. However, the average for the literature correlations is within 1% of the Kenics correlation and within 9% of the Fluent prediction.

Figure 7 shows a raster plot of the pressure at the element surface. The fluid moves from the right to the left. The right side of the picture shows the pressure at the front of the element, looking at the element. The left side of the picture shows the pressure at the back of the element, looking through the element. A high pressure region is found where the high speed core coming from the previous element impinges on the blade (top right, Figure 7). A low pressure region is found where the fluid leaves the element (top left, Figure 7). The difference between the minimum and maximum pressures at the element surface was 1.8 times the average pressure drop across the element.

Table 1 Parameters for equation (2). A, K_{ol} and K'_{ol} are Re dependent; the values listed here are for Re = 10 only.

L/D	Re	<w>	ρ	A	Kol	K'ol
9	10	0.01	1000	8.5	5.31	.0528

Table 2 Pressure drop across the six 180° elements.

	FLUENT	Kenics [7]	Wilkinson [1]	Pahl [2]	Kemblowski [3]	Bohnet [4]	Shaw [5]
Δp(Pa)	15.2	16.6	21.7	20.1	16.3	12.9	11.7
			Average Literature: 16.5 Pa				

III.C. Mixing

The transport of two chemical species, named white and black, was calculated. The binary diffusion coefficient of the two species was $D = 1.5\ 10^{-9}\ m^2/s$. The center of the inlet was 100% white; the outside of the inlet was 100% black as is shown in Fig. 8. The results are presented by means of raster plots, showing the concentration fields of the chemical species at various intersections in the tubes (Figures 9a,b,c,d).

Figures 9a,b,c show the concentration fields after 18°, 54°, 90°, 126° and 162° degrees rotation in the first, second and third 180° mixing element respectively. Figure 9d shows a similar concentration field in the sixth element.

Figure 9a shows how the white core coming from the inlet is split into two white islands. The two white islands are stretched and move outward. The black, which was on the outside in the inlet of the element is split in two semi-circular filaments, which are moved towards the inside of the element.

The second element splits the two white islands, forming four white islands, all located in the corners near the blade. The two black zones are split in four zones too, but since these were located near the centerline they merge two by two. This again results in two black zones. Within the element the two black islands are moved to the center.

After the flow division at the inlet of the third element the light grey zones in the corners join. When we compare the concentration profiles at 18° in the third element with the profile at 18° in the first element we see that we now have a mainly black core in the center instead of a mainly white core. The highest concentrations of white are now found at the outside. The splitting and stretching process in the first two elements has resulted in a concentration field which looks like it is flipped inside-out.

This process of splitting, stretching, folding and flipping inside out repeats itself every two elements, until the fluids are mixed. By the time the end of the sixth element is reached (Fig. 9d), the species concentrations are nearly uniform.

IV. CONCLUSIONS

The current state of the art in CFD allows for the modelling of flows and mixing of chemical species in complex geometries like the Kenics mixing element. Drawbacks, however, are the excessive computation times and the fact that the models need extensive manual tuning before they converge. However, even though the simulations are computer time intensive, optimizing the geometry of the mixing elements for a variety of operating conditions, fluid viscosities, equipment size etc. can be done faster this way than by conducting an extensive experimental program.

The Kenics design procedures predict a 10% higher pressure drop than the CFD simulations do, thus allowing for a safety margin.

The Fluent results indicate that, despite common belief, in laminar flow there is no real circulation in a helical element. There is, however, a relative motion between the fluid and the mixing element due to the twist of the element, which in the past may have been misinterpreted as real circulation.

The flow pattern and mixing of a chemical species in a tube equipped with Kenics elements was calculated to evaluate the mixing mechanism. Mixing occurs through a

combination of flow splitting and shearing at the junctions of successive elements and a stretching and folding mechanism within the elements. The concentration field looks like it is flipped inside out after two elements: material originally at the wall is in the core and vice versa. This makes the Kenics element an excellent radial mixing device, applicable in a variety of laminar mixing applications.

V. RECOMMENDATIONS AND POSSIBLE FUTURE WORK

These computations were done for a Reynolds number of Re = 10 and tubes being 0.02 m in diameter. It will be useful to perform similar simulations for a wider range of geometries and operating conditions to verify the conclusions drawn above.

Future work could also include the calculation of heat transfer coefficients. This is relatively straightforward now that the models for the simulation of the flow patterns have been developed.

VI. LITERATURE

1. Wilkinson W.L., Cliff M.J. (1977)
   An Investigation into the Performance of a Static In-Line Mixer
   Proceedings Second European Conference on Mixing, 30th March - 1st April, 1977, Held at St John's College, Cambridge, England
2. Pahl, Muschelknautz (1979)
   Chem.-Ing.-Techn., 51, No. 5, p.347
3. Kemblowski Z., Pustelnik P., Frontczak, Julianski (1976)
   Reszyty Naukow Politechniki Lodzkiej, Inzynieria Chemiczne, No. 6, p. 29
4. Bohnet M., Calvetz H. (1990)
   Symp. "25 Years of Static Mixing", 16-17 October, Aachen, Germany
5. Shaw N.F., Kale D.D. (1991)
   Pressure Drop for Laminar Flow of Non-Newtonian Fluids in Static Mixers
   Chem.Eng.Sci., Vol. 46, No. 8, p2159-2161
6. Fluent V4 Users Manual (1991)
   Users Guide
7. Kenics Static Mixers KTEK-Series (1988)
   Chemineer, Inc., Internal Report

VII. SYMBOLS

D	Tube diameter (m)
D	Diffusion coefficient (m^2/s)
l	Length of a helical element (m)
L	Length of array of helical elements (m)
Δp	Pressure drop (Pa)
Re	Reynolds number (-)
T	Twist of the blade (radians)
u	Velocity in x-direction (m)
v	Velocity in y-direction (m)
w	Velocity in z-direction (m)
<w>	Average normal velocity in a plane (m/s)
x	X-coordinate (m)
y	Y-coordinate (m)
z	Axial coordinate (m)

VIII. LIST OF FIGURES

Figure 1

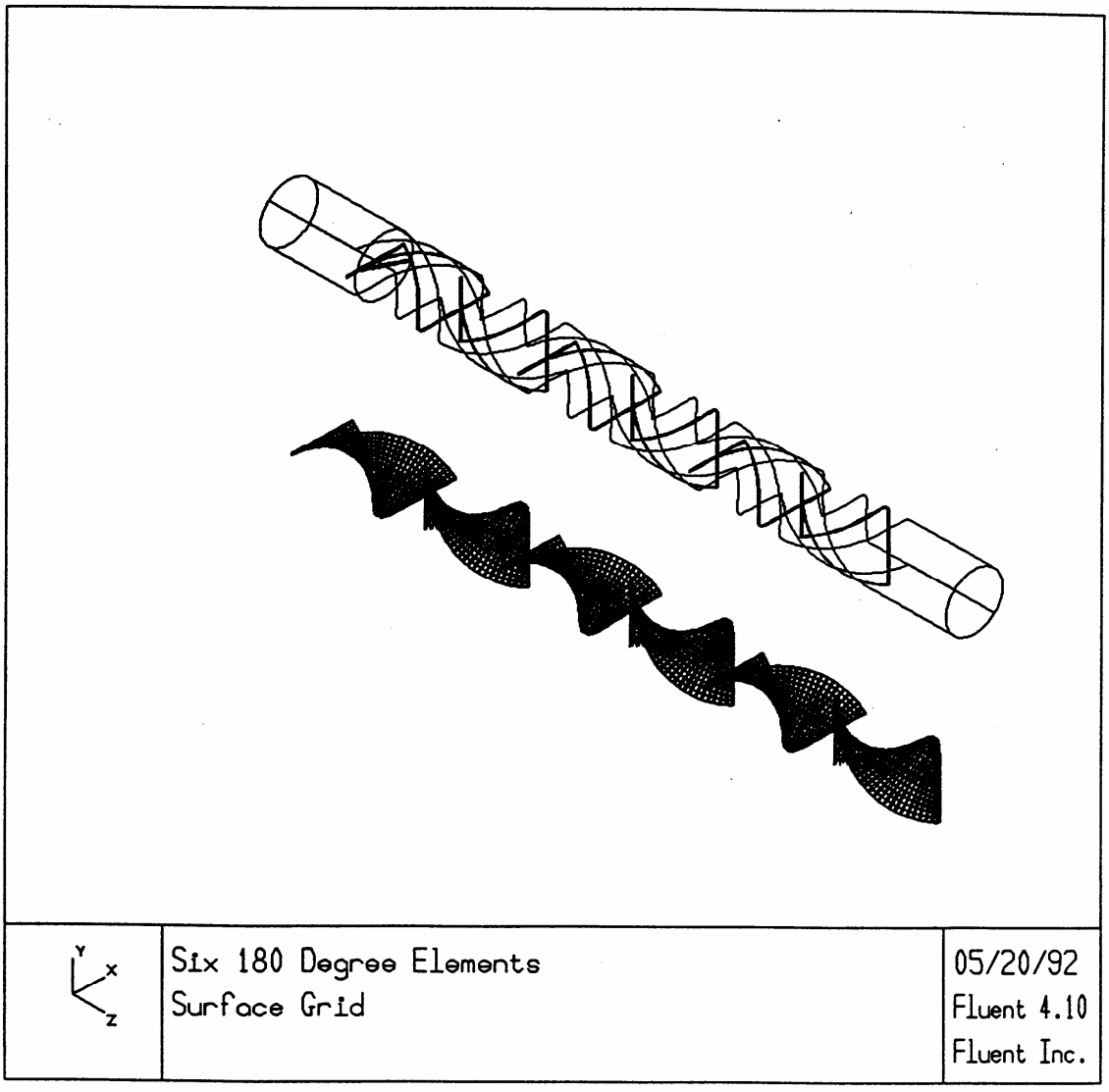
Y
X
Z
Six 180 Degree Elements
Surface Grid
05/20/92
Fluent 4.10
Fluent Inc.

Figure 2

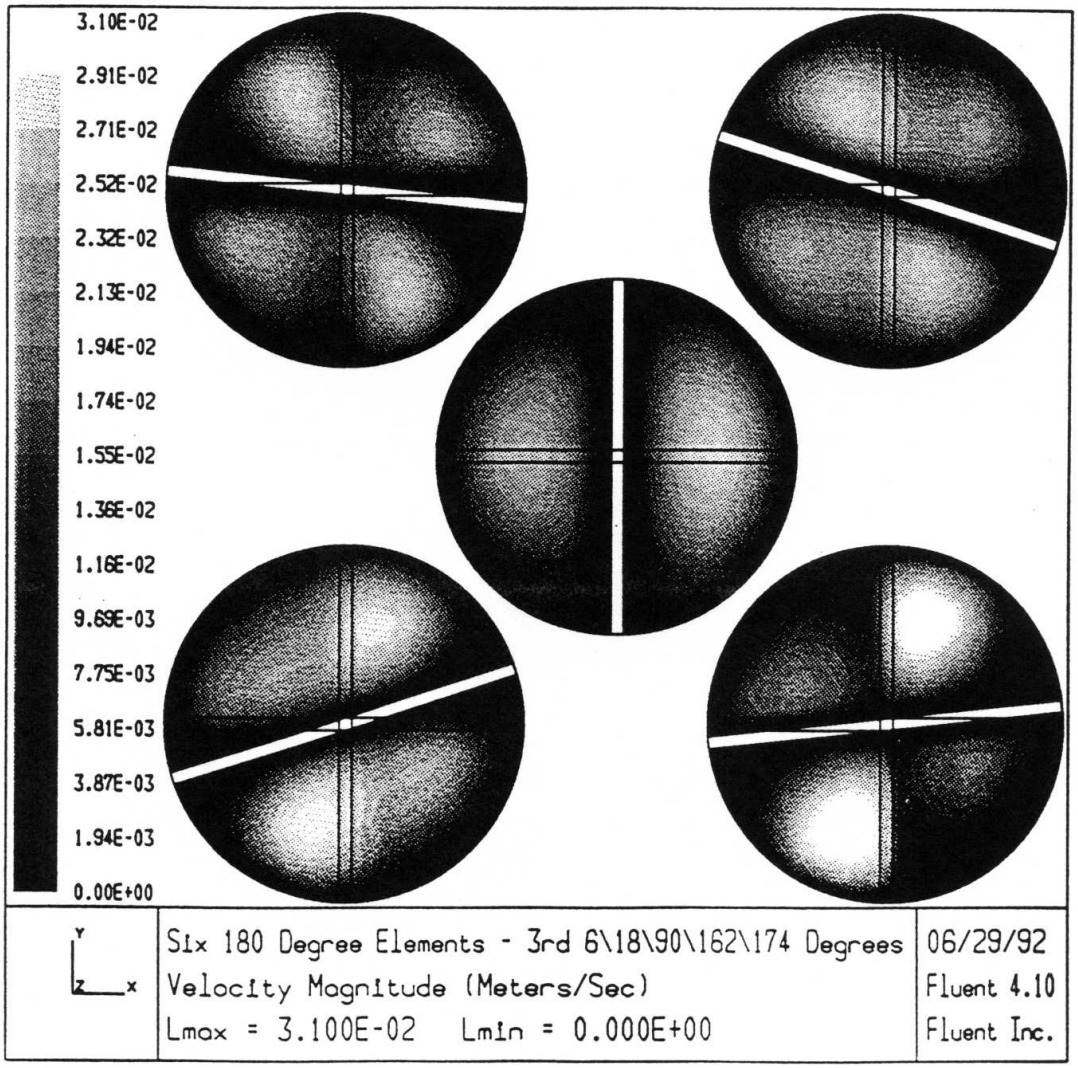
3.10E-02
2.91E-02
2.71E-02
2.52E-02
2.32E-02
2.13E-02
1.94E-02
1.74E-02
1.55E-02
1.36E-02
1.16E-02
9.69E-03
7.75E-03
5.81E-03
3.87E-03
1.94E-03
0.00E+00
Y
Z
X
Six 180 Degree Elements - 3rd 6\18\90\162\174 Degrees
Velocity Magnitude (Meters/Sec)
Lmax = 3.100E-02 Lmin = 0.000E+00
06/29/92
Fluent 4.10
Fluent Inc.

Figure 3a

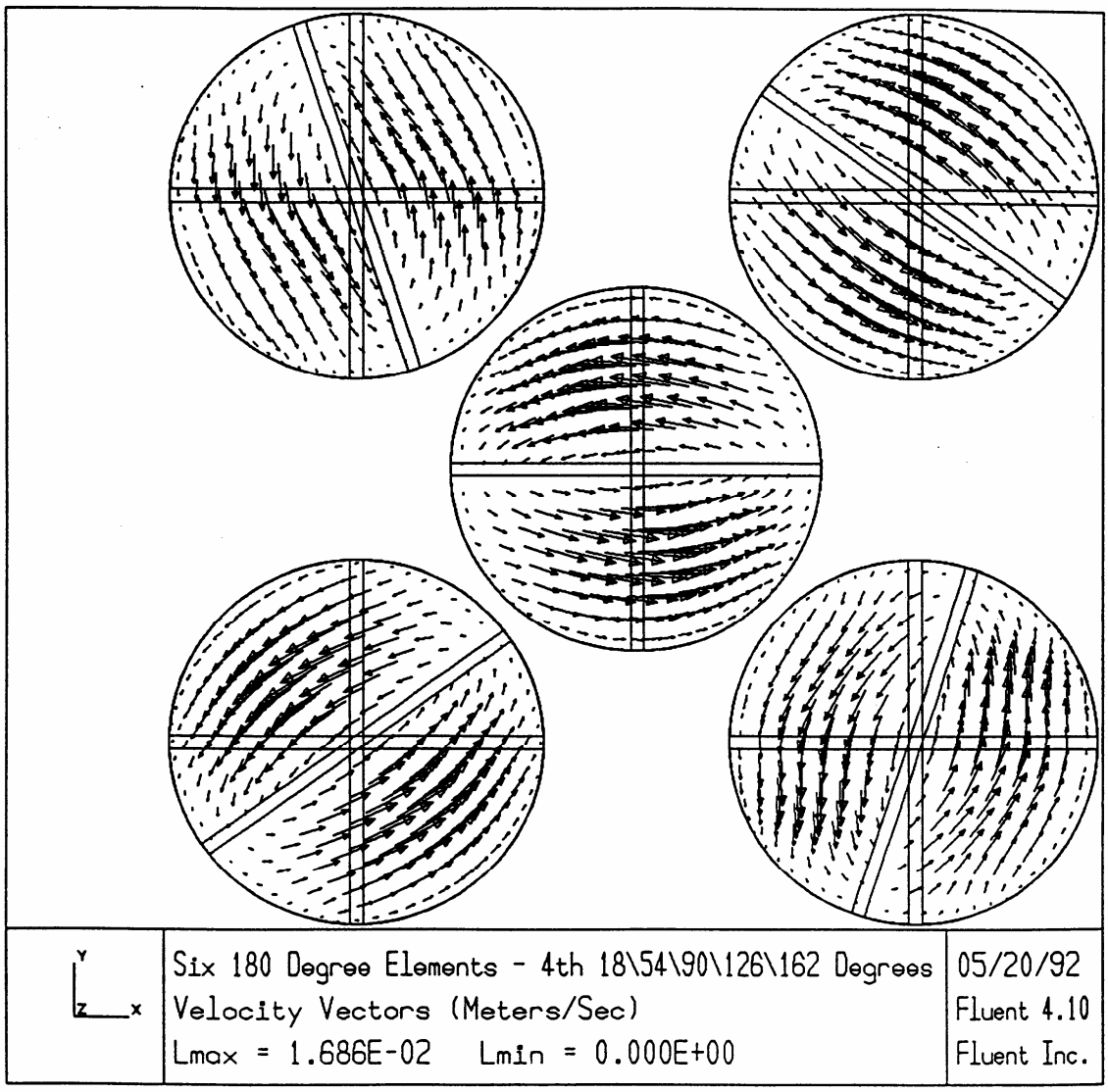
Y
Z
X
Six 180 Degree Elements - 4th 18\54\90\126\162 Degrees
Velocity Vectors (Meters/Sec)
Lmax = 1.686E-02 Lmin = 0.000E+00
05/20/92
Fluent 4.10
Fluent Inc.

Figure 3b

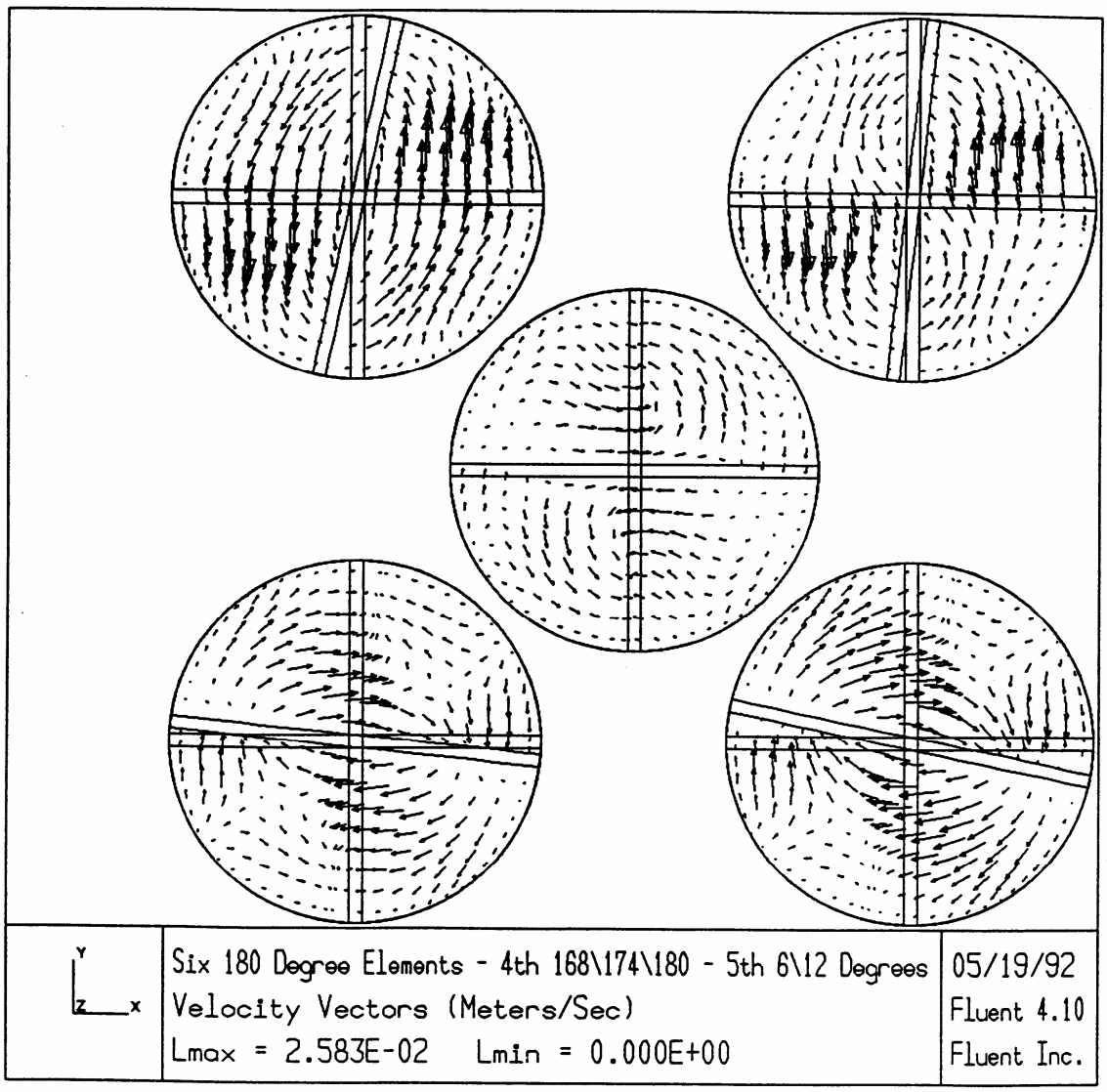
Y
Z
X
Six 180 Degree Elements - 4th 168\174\180 - 5th 6\12 Degrees
Velocity Vectors (Meters/Sec)
Lmax = 2.583E-02 Lmin = 0.000E+00
05/19/92
Fluent 4.10
Fluent Inc.

Figure 4

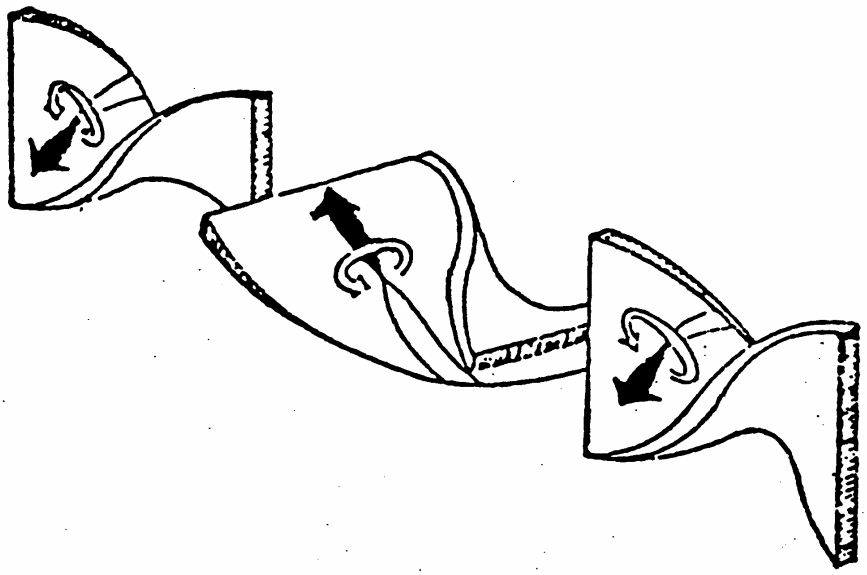

Diagram of Kenics in-line mixer

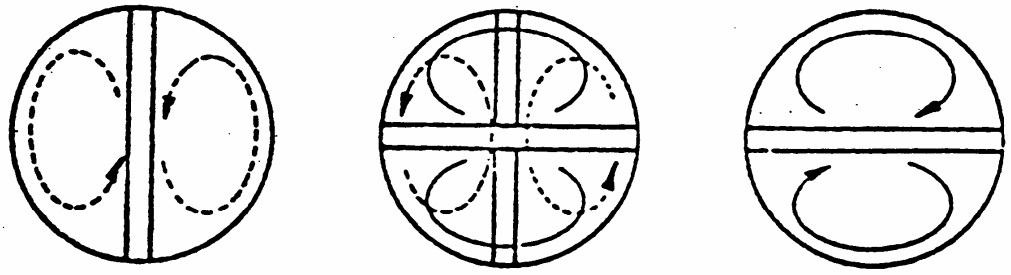

Secondary flow in the in-line mixer

Figure 5

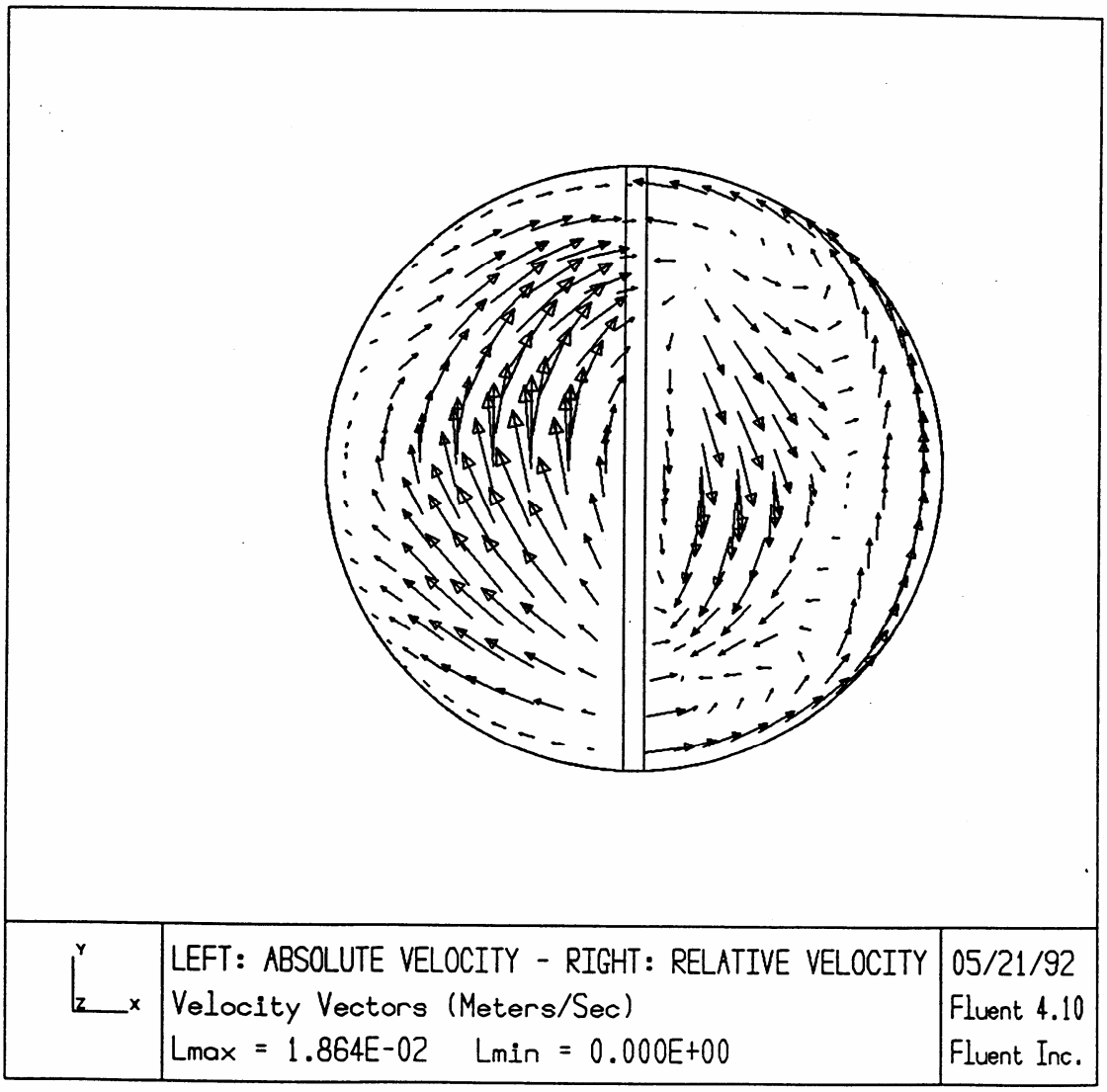
Y
Z
X
LEFT: ABSOLUTE VELOCITY - RIGHT: RELATIVE VELOCITY
Velocity Vectors (Meters/Sec)
Lmax = 1.864E-02 Lmin = 0.000E+00
05/21/92
Fluent 4.10
Fluent Inc.

Figure 6

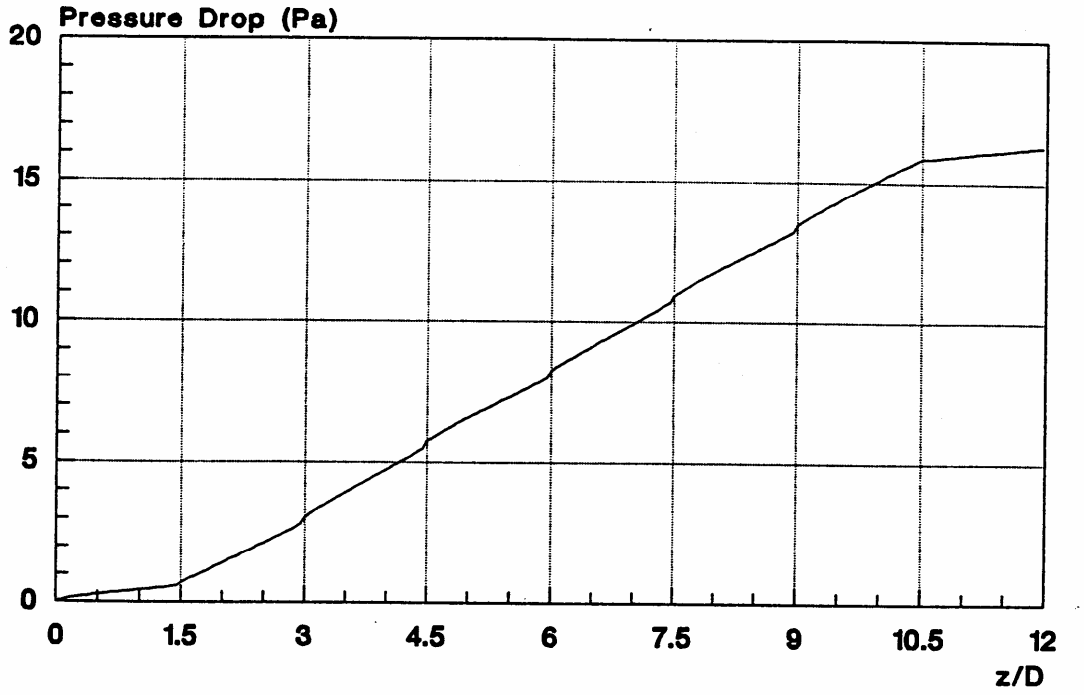

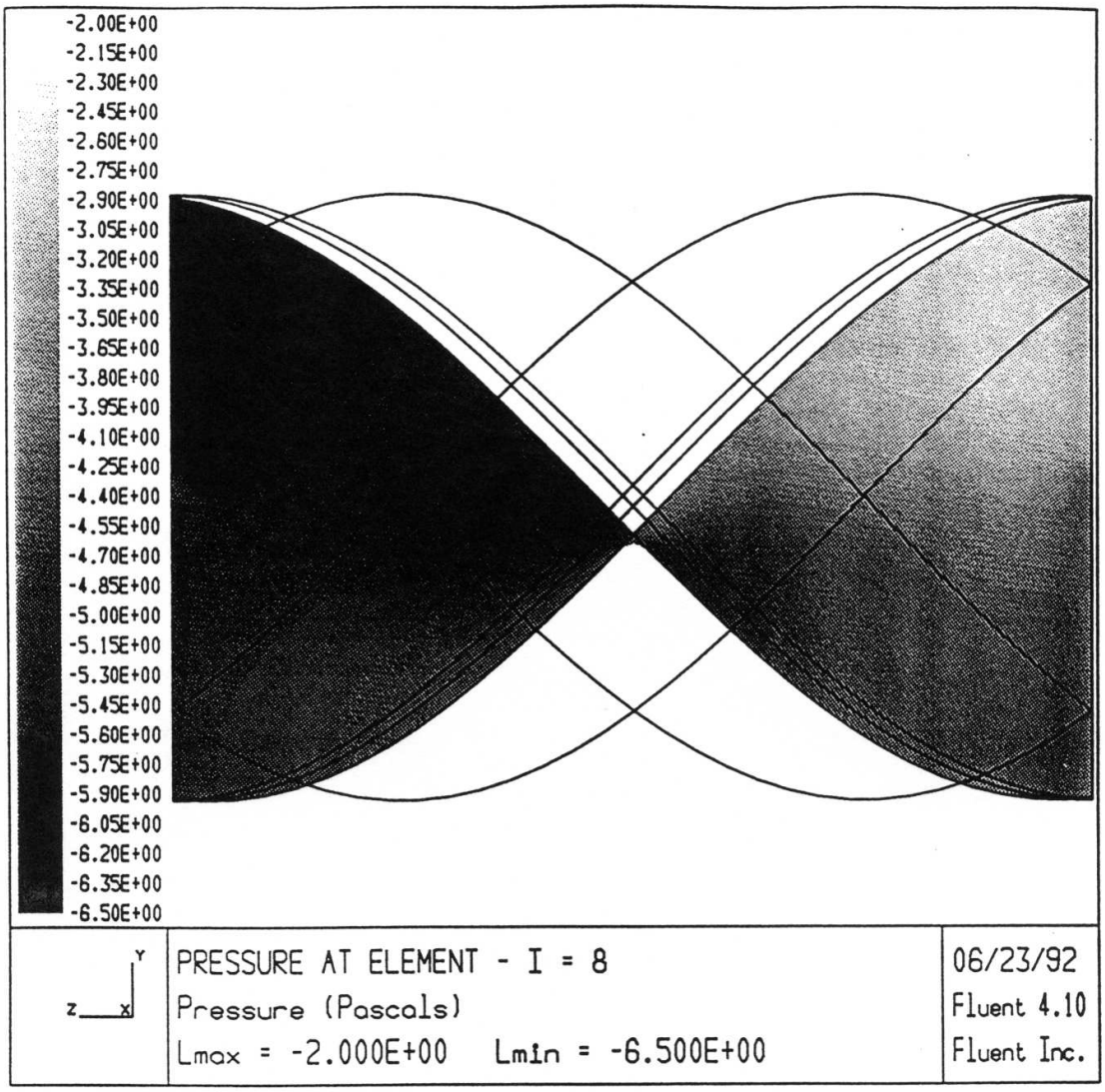
-2.00E+00
-2.15E+00
-2.30E+00
-2.45E+00
-2.60E+00
-2.75E+00
-2.90E+00
-3.05E+00
-3.20E+00
-3.35E+00
-3.50E+00
-3.65E+00
-3.80E+00
-3.95E+00
-4.10E+00
-4.25E+00
-4.40E+00
-4.55E+00
-4.70E+00
-4.85E+00
-5.00E+00
-5.15E+00
-5.30E+00
-5.45E+00
-5.60E+00
-5.75E+00
-5.90E+00
-6.05E+00
-6.20E+00
-6.35E+00
-6.50E+00
Y
z
x
PRESSURE AT ELEMENT - I = 8
Pressure (Pascals)
Lmax = -2.000E+00 Lmin = -6.500E+00
06/23/92
Fluent 4.10
Fluent Inc.

Figure 7

Figure 8

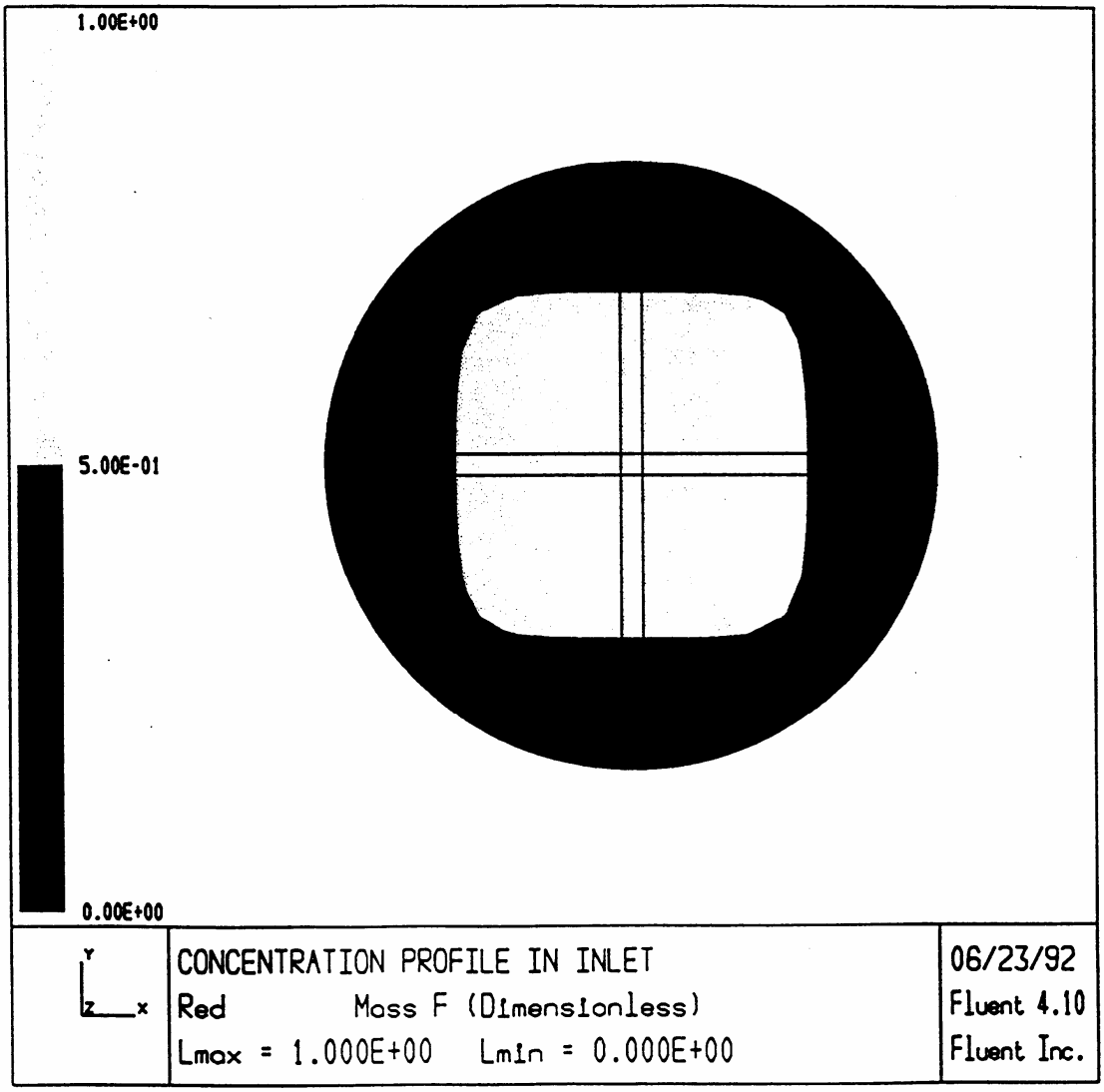
1.00E+00
5.00E-01
0.00E+00
Y
Z
X
CONCENTRATION PROFILE IN INLET
Red Mass F (Dimensionless)
Lmax = 1.000E+00 Lmin = 0.000E+00
06/23/92
Fluent 4.10
Fluent Inc.

Figure 9a

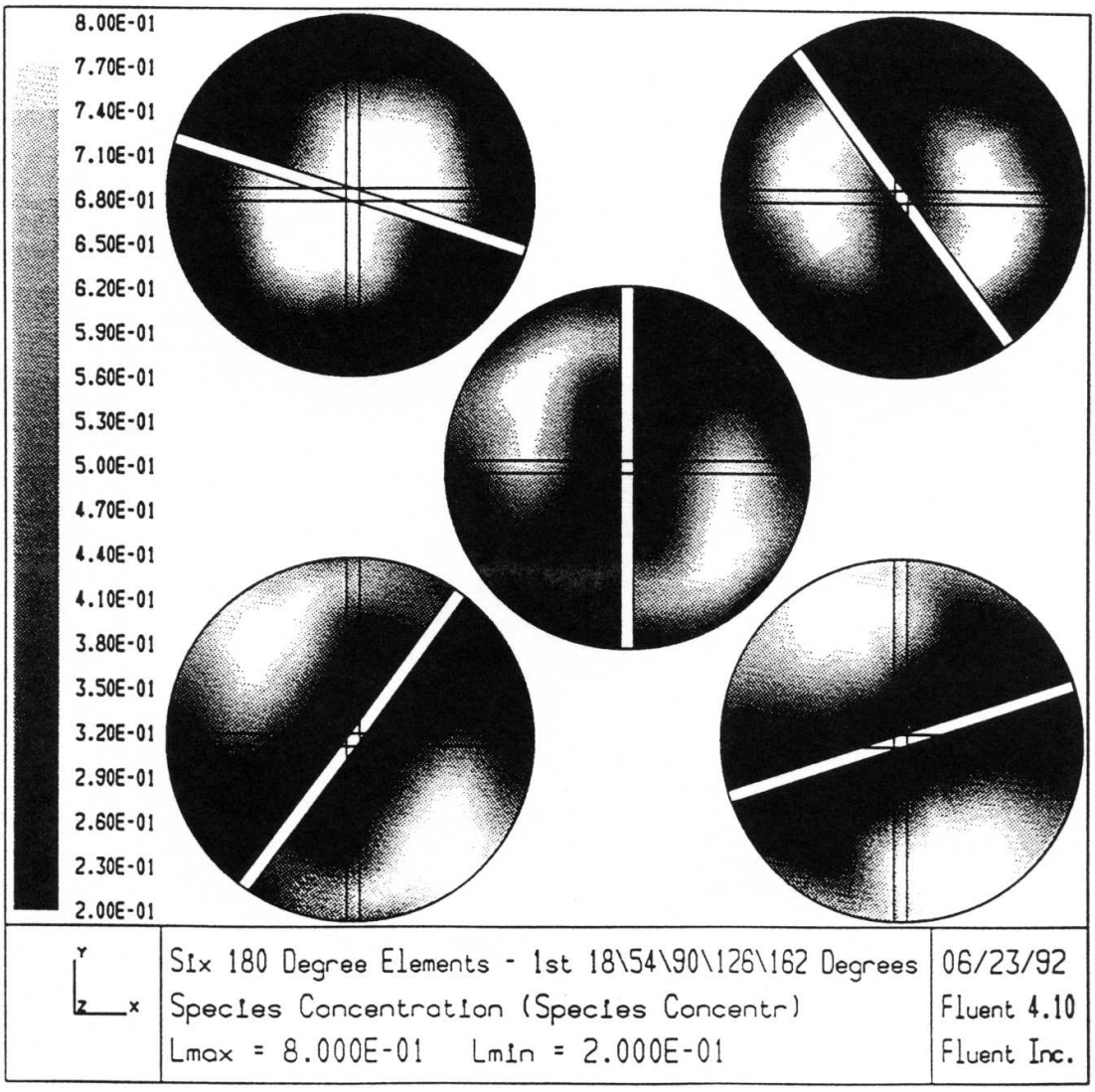
8.00E-01
7.70E-01
7.40E-01
7.10E-01
6.80E-01
6.50E-01
6.20E-01
5.90E-01
5.60E-01
5.30E-01
5.00E-01
4.70E-01
4.40E-01
4.10E-01
3.80E-01
3.50E-01
3.20E-01
2.90E-01
2.60E-01
2.30E-01
2.00E-01
Y
Z
X
Six 180 Degree Elements - 1st 18\54\90\126\162 Degrees
Species Concentration (Species Concentr)
Lmax = 8.000E-01 Lmin = 2.000E-01
06/23/92
Fluent 4.10
Fluent Inc.

Figure 9b

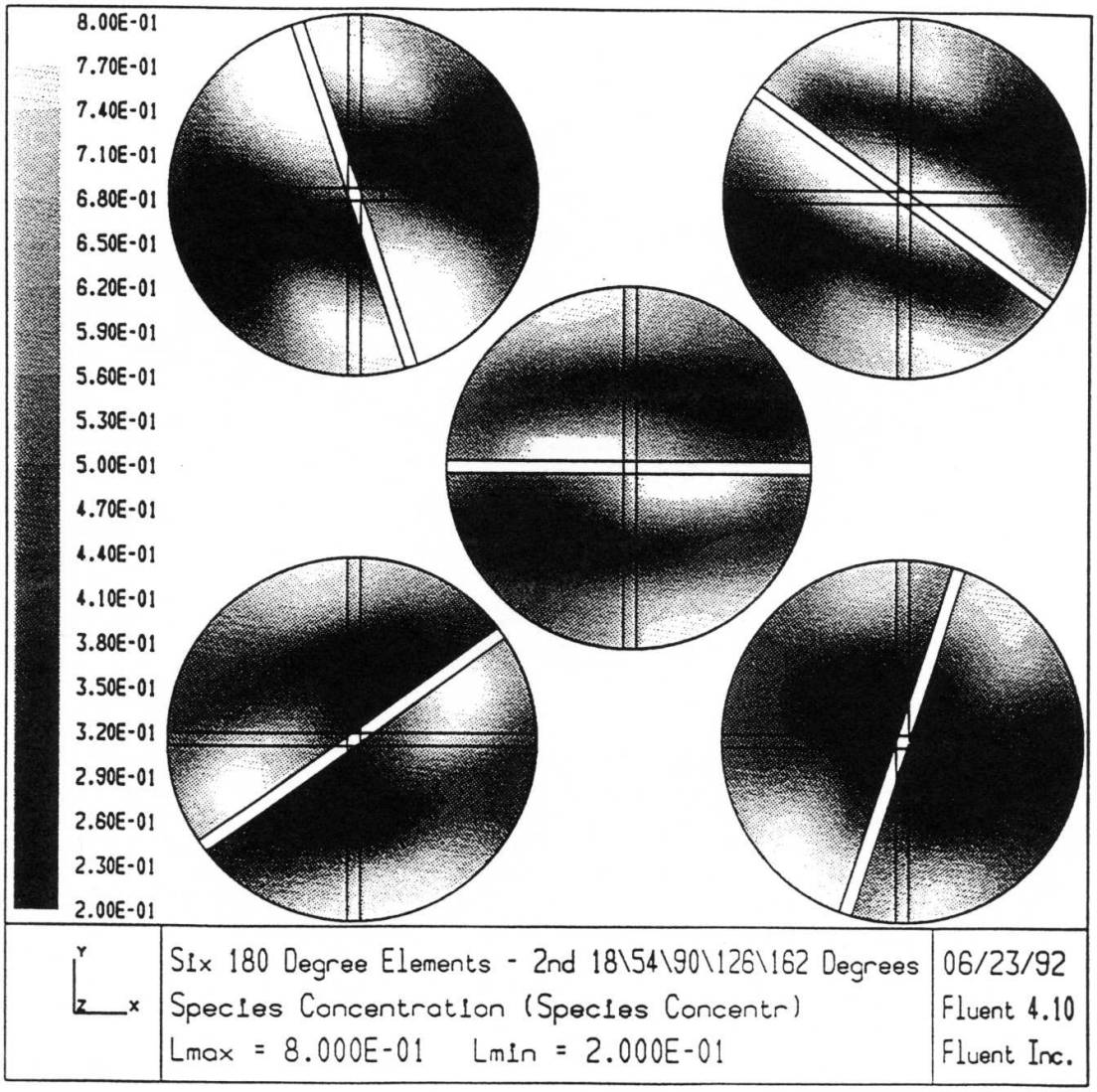
8.00E-01
7.70E-01
7.40E-01
7.10E-01
6.80E-01
6.50E-01
6.20E-01
5.90E-01
5.60E-01
5.30E-01
5.00E-01
4.70E-01
4.40E-01
4.10E-01
3.80E-01
3.50E-01
3.20E-01
2.90E-01
2.60E-01
2.30E-01
2.00E-01
Y
Z
X
Six 180 Degree Elements - 2nd 18\54\90\126\162 Degrees
Species Concentration (Species Concentr)
Lmax = 8.000E-01 Lmin = 2.000E-01
06/23/92
Fluent 4.10
Fluent Inc.

Figure 9c

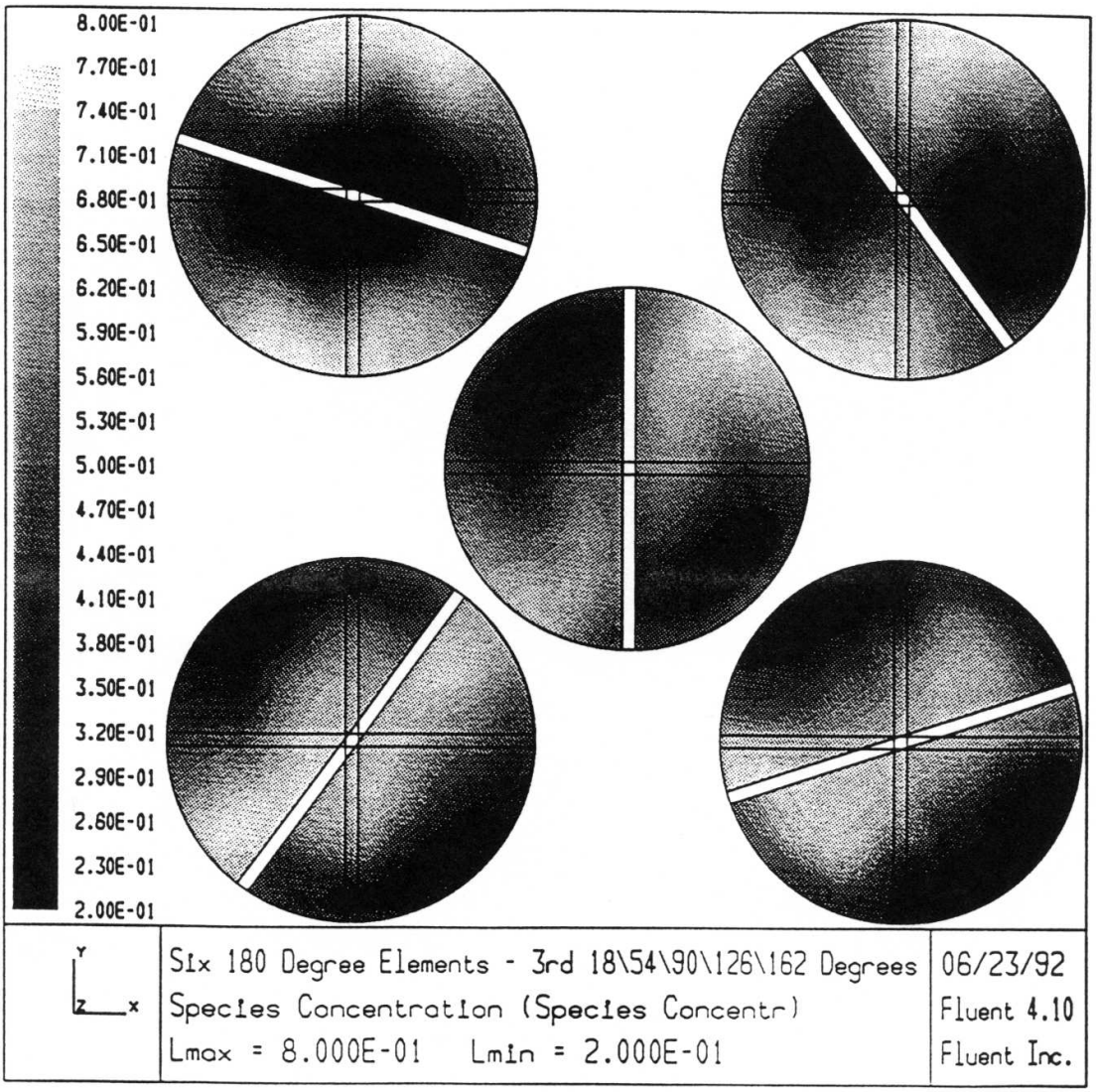
8.00E-01
7.70E-01
7.40E-01
7.10E-01
6.80E-01
6.50E-01
6.20E-01
5.90E-01
5.60E-01
5.30E-01
5.00E-01
4.70E-01
4.40E-01
4.10E-01
3.80E-01
3.50E-01
3.20E-01
2.90E-01
2.60E-01
2.30E-01
2.00E-01
Y
Z
X
Six 180 Degree Elements - 3rd 18\54\90\126\162 Degrees
Species Concentration (Species Concentr)
Lmax = 8.000E-01 Lmin = 2.000E-01
06/23/92
Fluent 4.10
Fluent Inc.

Figure 9d

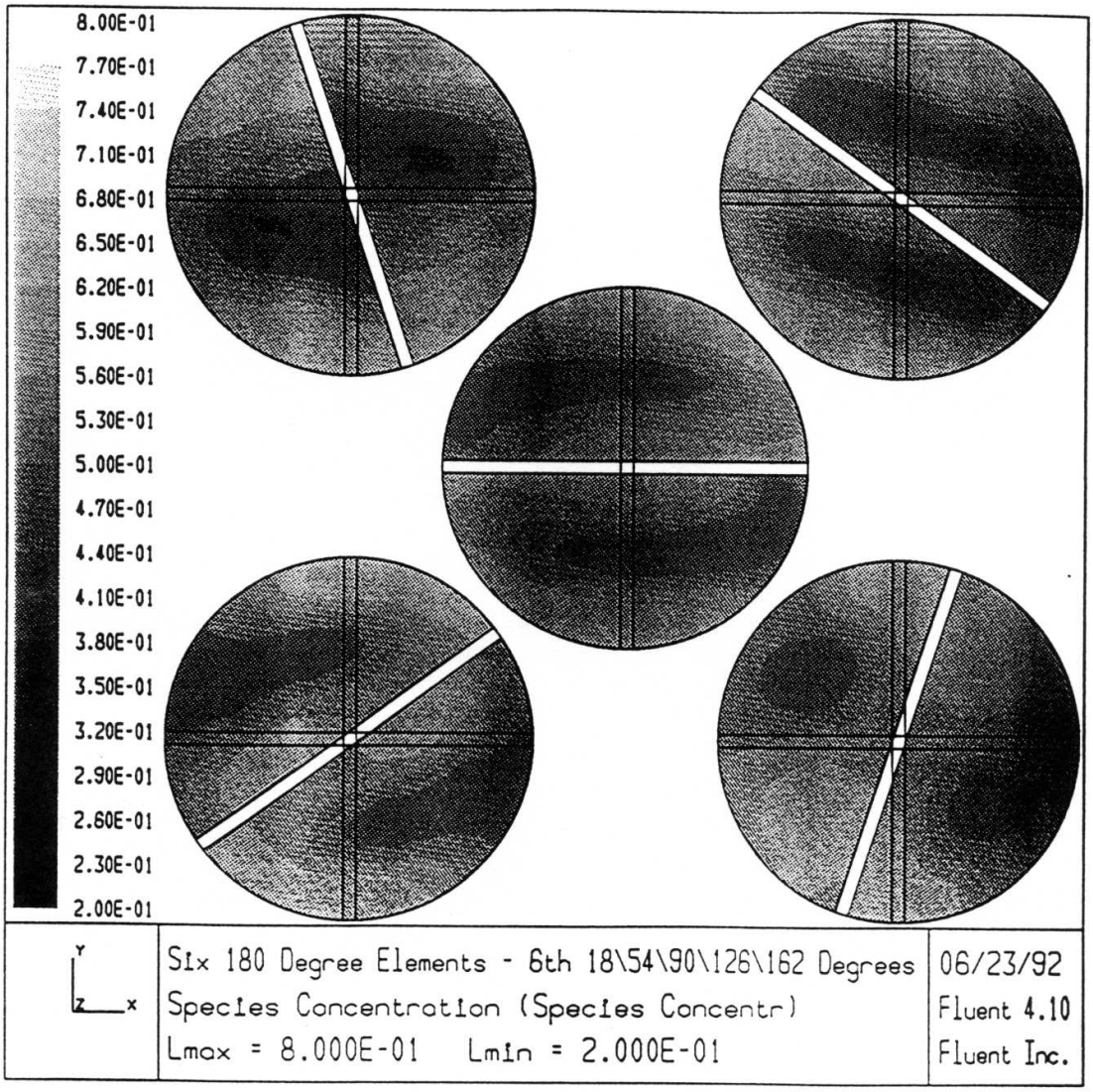
8.00E-01
7.70E-01
7.40E-01
7.10E-01
6.80E-01
6.50E-01
6.20E-01
5.90E-01
5.60E-01
5.30E-01
5.00E-01
4.70E-01
4.40E-01
4.10E-01
3.80E-01
3.50E-01
3.20E-01
2.90E-01
2.60E-01
2.30E-01
2.00E-01
Y
Z
X
Six 180 Degree Elements - 6th 18\54\90\126\162 Degrees
Species Concentration (Species Concentr)
Lmax = 8.000E-01 Lmin = 2.000E-01
06/23/92
Fluent 4.10
Fluent Inc.